Carbon dioxide transport in alligator blood and its erythrocyte permeability to anions and water

FRANK B. JENSEN,[1] TOBIAS WANG,[1] DAVID R. JONES,[2] AND JESPER BRAHM[3]
[1]*Institute of Biology, Odense University, DK-5230 Odense M;* [3]*Department of Medical Physiology, The Panum Institute, Copenhagen University, DK-2200 Copenhagen N, Denmark; and* [2]*Department of Zoology, University of British Columbia, Vancouver, V6T 1Z4 Canada*

Jensen, Frank B., Tobias Wang, David R. Jones, and Jesper Brahm. Carbon dioxide transport in alligator blood and its erythrocyte permeability to anions and water. *Am. J. Physiol.* 274 (*Regulatory Integrative Comp. Physiol.* 43): R661–R671, 1998.—Deoxygenation of alligator red blood cells (RBCs) caused binding of two HCO_3^- equivalents per hemoglobin (Hb) tetramer at physiological pH. At lowered pH, some HCO_3^- binding also occurred to oxygenated Hb. The erythrocytic total CO_2 content was large, and Hb-bound HCO_3^-, free HCO_3^-, and carbamate contributed about equally in deoxygenated cells. The nonbicarbonate buffer values of RBCs and Hb were high, and the Hb showed a significant fixed acid Haldane effect. Binding of HCO_3^- on deoxygenation occurred without a change in RBC intracellular pH, revealing equivalence between oxylabile HCO_3^- and H^+ binding. Erythrocyte volume, plasma pH, and plasma HCO_3^- concentration also varied little with the degree of oxygenation. Diffusional water permeability was higher in oxygenated than deoxygenated RBCs. The RBCs have rapid band 3-mediated Cl^- and HCO_3^- transport, which was not affected by degree of oxygenation, but net fluxes of Cl^- and HCO_3^- via the anion exchanger are small during blood circulation at rest. Most of the CO_2 taken up into the blood as it flows through tissue capillaries is carried within the erythrocytes as Hb-bound HCO_3^- until CO_2 is excreted when blood flows through pulmonary capillaries.

allosteric binding of bicarbonate; red cell anion exchange; Haldane effect; blood CO_2 transport; crocodiles

THE HEMOGLOBIN (Hb) of crocodiles is unique compared with other vertebrate Hbs by showing an oxygenation-linked binding of bicarbonate ions (1). Bicarbonate binds to the deoxy (T) structure of the Hb at the entrance to the central cavity between the two β-chains; i.e., the site involved in organic phosphate binding in other vertebrate Hbs (21). A few amino acid substitutions in crocodile Hbs have made the binding site incompatible with organic phosphate and compatible with the binding of two HCO_3^- ions (19, 21). The allosteric binding of HCO_3^- underlies the large effect of CO_2 on blood-Hb O_2 affinity seen in crocodiles (1, 2, 12, 28). As noted by Perutz and co-workers (21), the oxygenation-linked binding of HCO_3^- gives a simple and direct reciprocal action between O_2 and one of the end products of oxidative metabolism. The mechanism has, however, not been adopted by other vertebrates and it is unknown what significance it may have for the crocodilians (21). A link between O_2 and metabolically produced CO_2 (that after hydration forms HCO_3^- and H^+) is also present in other vertebrates through the oxylabile binding of H^+ to Hb (the fixed acid Bohr-Haldane effect).

Whereas the molecular mechanism of bicarbonate binding and the effects of CO_2 on Hb O_2 affinity are well documented in crocodiles, the consequences of the special functional properties of crocodile Hbs have remained largely unexplored at the red blood cell (RBC) level. This particularly applies to CO_2 transporting properties. Hb is important for both O_2 and CO_2 transport in the blood. The functional significance of HCO_3^- binding may therefore equally well be related to its consequences for CO_2 transport as it may be related to its effects on O_2 affinity. Bicarbonate binding to Hb can be predicted to provide crocodile RBCs with unique CO_2 transporting properties, where the fraction of total blood CO_2 contained within the RBCs is larger than in other vertebrates. In the normal vertebrate CO_2 transport pattern, two processes drive the CO_2 hydration reaction in the RBCs toward bicarbonate formation. These are H^+ binding to the Hb and a shift of produced HCO_3^- to the plasma in exchange for Cl^- via the anion exchanger (known as AE1 or band 3). In crocodiles, bicarbonate binding to Hb provides an additional mechanism of removing free HCO_3^- from the RBC cytosol, increasing the amount of CO_2 that is hydrated and thereby the blood CO_2 carrying capacity. Anion exchange is generally considered the rate-limiting step in the uptake of CO_2 in tissue capillaries and the excretion of CO_2 across the respiratory epithelium. This particularly applies if band 3 transport capacity and/or velocity is reduced. On this basis, it is possible that oxygenation-linked HCO_3^- binding has evolved in crocodiles to compensate for a slow HCO_3^-/Cl^- exchange across the RBC membrane.

Oxygenation-linked binding of bicarbonate can also be expected to have consequences for RBC acid-base status and the nonpermeable charge carried by the Hb molecule, so that the influence of oxygenation on RBC intracellular pH (pH_i) and on the Donnan-like distribution of permeable ions across the RBC membrane in crocodiles should be different from other vertebrates.

The present study was designed to investigate these ideas in the alligator, *Alligator mississippiensis*. Specifically, we have *1*) traced the unique allosteric HCO_3^- binding to the RBC level, *2*) analyzed the influences of CO_2 and of oxygenation on extra- and intracellular acid-base status, *3*) studied CO_2 and H^+ binding properties of blood and Hb, *4*) made a partitioning of various forms of CO_2 in erythrocytes, and *5*) determined the Cl^-, HCO_3^-, and H_2O permeability of the RBC membrane.

MATERIALS AND METHODS

Alligators (*A. mississippiensis*, 1.2–1.7 m in length, $n = 6$) were kept at 30°C in a 20-m^2 room with facilities for basking

and immersion in water. They were fed chicken once a week and dry dog food (pellets) ad libitum. One to two days before blood sampling, a catheter was inserted occlusively in the femoral artery of one of the hindlegs under local anesthesia (Xylocaine). The animals were then placed individually in a box, which was partly covered with a blanket to allow sampling of blood without disturbing the animal. Approximately 40 ml of blood was drawn from the femoral artery of each animal. The first 10 ml was used for blood tonometry and the remaining 30 ml was used for flux experiments.

Blood Tonometry

Blood was equilibrated in Eschweiler (Kiel, Germany) tonometers to humidified gas mixtures containing 2, 4, and 7% CO_2 (P_{CO_2} values of 14.5, 29, and 50.8 mmHg, respectively) with air (oxygenated blood; P_{O_2}: 141.9–149.5 mmHg) or N_2 (deoxygenated blood) as balance. Gas mixtures were delivered from Wösthoff (Bochum, Germany) gas mixing pumps. Two tonometers, both set at 30°C, were run in parallel. One was used for oxygenated blood and the other for deoxygenated blood. At each CO_2 and oxygenation level, 1.2 ml of blood was equilibrated for 45 min. A 600-μl sample was drawn into an Eppendorf tube and used for measurement of blood pH, blood Hb, hematocrit (Hct), and number of RBCs (N_{RBC}). Blood remaining in the tube was centrifuged, and the plasma was used for measurement of total CO_2 (C_T) and lactate in true plasma. The packed RBCs were frozen (in liquid N_2) and thawed twice, whereupon RBC pH was measured on the lysate. An additional 600-μl blood sample was then drawn from the tonometer into a dried and preweighed Eppendorf tube. Thirty microliters was used for measurement of whole blood C_T, whereafter the tube was centrifuged. The plasma was discharged, and the wet weight of the RBCs was determined. The RBCs were then dried at 105°C overnight for determination of dry weight. The fractional water content of the RBCs (F_{H_2O}) was determined from the wet and dry masses.

Extracellular blood pH (pH_e) and RBC pH_i were measured with a Radiometer (Copenhagen, Denmark) capillary pH electrode and a Radiometer PHM 73 monitor. Hb was measured spectrophotometrically after conversion of Hb to cyanmethemoglobin using a millimolar extinction coefficient of 11 at 540 nm. Hct was assessed by centrifugation in glass capillaries. The red cell Hb concentration ([Hb]) was calculated from blood [Hb] and Hct. N_{RBC} counts were performed using a Bürger-Türk counting chamber and a microscope. Mean cellular volume (MCV) was calculated from Hct/N_{RBC}. Plasma lactate was assessed with the Boehringer-Mannheim lactate dehydrogenase method. C_T values in plasma and in whole blood were measured with the Cameron (8) method. Plasma bicarbonate was calculated as plasma C_T (C_T^{plasma}) − (α_{CO_2})P_{CO_2}, using a plasma CO_2 solubility (α_{CO_2}) at 30°C of 0.0366 mmol·l^{-1}·mmHg^{-1} [calculated from the formula of Heisler (14) and the concentrations of ions in alligator plasma (11)]. The apparent RBC bicarbonate concentration ($[HCO_3^-]_{app}$; in mmol/l RBC) was calculated from blood and plasma C_T and the fractional Hct (F_{Hct}), according to the formula

$$\text{red cell } [HCO_3^-]_{app} = \{[C_T^{blood} - (1 - F_{Hct})C_T^{plasma}]/F_{Hct}\} - \alpha_{CO_2}P_{CO_2}$$

using an RBC α_{CO_2} value of 0.032 mmol·l^{-1}·mmHg^{-1} (extrapolated from human values; Ref. 23). The calculated quantity is an $[HCO_3^-]_{app}$, as it also includes Hb-bound $[HCO_3^-]$ and carbamino compounds. $[HCO_3]_{app}$ values were converted to concentrations in millimoles per liter (cell water) using the corresponding red cell F_{H_2O} values.

The apparent pK′ for the CO_2/HCO_3^- system in alligator plasma at 30°C was calculated from measured plasma C_T and pH values, using the rearranged Henderson-Hasselbalch equation

$$pK' = pH - \log[(C_T/\alpha_{CO_2}P_{CO_2}) - 1]$$

Linear regression on the data gave the following relationship between pK′ and pH for alligator plasma: pK′ = −0.0817 × pH + 6.7818.

Data from blood tonometry are presented as means ± SE, and the significance of differences between treatments were evaluated by a two-factor (oxygenation degree and CO_2 level) analysis of variance (ANOVA) (repeated-measures design) followed by the Tukey multiple-comparison test.

Flux Measurements

Freshly drawn blood was centrifuged, the buffy coat was sucked off, and the RBCs were washed three times in a physiological saline with the following composition (in mmol/l): 106 NaCl, 25 $NaHCO_3$, 2.5 KH_2PO_4, 2 $CaCl_2$, 1 $MgSO_4$, 3.9 glucose, and 10 *N*-2-hydroxyethylpiperazine-*N*′-2-ethanesulfonic acid buffer. After the last wash, the cells were resuspended in the saline to a Hct of ~40%. Suspension pH was typically 7.6. Five-milliliter samples were equilibrated in an Eschweiler tonometer for 45 min at 30°C with either air (to oxygenate the RBCs) or N_2 (to deoxygenate the RBCs). After the incubation, the cells were prepared by a procedure slightly modified from that described previously (4, 6). Each sample was spun down, the Hct was increased to 60% (to save isotope), and isotope, $^{36}Cl^-$, $[^{14}C]HCO_3^-$, ^3H_2O, or $[^{14}C]HCO_3^-$ + ^3H_2O, was added to the supernatant before mixing again with the cells to achieve isotopic equilibrium. The final radioactivity for each isotope was 3.7–18.5 kBq (0.1–0.5 μCi)/ml cell suspension. The cells stood for 1–2 min, which by far exceeds the time for the rapid equilibration at room temperature. The cells were sufficiently packed by centrifugation at 5,000 *g* for 10 min because of the large size of alligator RBCs (the volume is 4× that of human RBCs). Furthermore, it has been shown that the Hct of the packed RBC sample for the efflux experiment has no effect on the slope of the efflux curves (6). In some experiments the anion transport inhibitors 4,4′-dinitrostilbene-2,2′-disulfonate (DNDS, final concentration 2.5 mM) or phloretin (final concentration 30 μM) were added to both the cell sample and the efflux media.

The rate of tracer efflux was determined at 30°C by means of the continuous flow tube technique that has a time resolution in milliseconds and therefore is well-suited to measure RBC anion transport (4, 6). In brief, 0.5 ml of the packed and radioactive loaded RBCs was continuously mixed with 270 ml of isotope-free saline in a mixing chamber. The saline was air equilibrated in experiments with oxygenated RBCs and N_2 equilibrated in experiments with deoxygenated RBCs. The dilute suspension flowed through a pipe where cell-free filtrates were collected at predetermined distances. The filtrates contained increasing amounts of radioactivity with increasing distance from the mixing chamber. With known flow rates, distances could be converted to times. Because tracer efflux follows a monoexponential course, plotting the extracellular radioactivity versus time in a semilogarithmic plot allowed a determination of the rate of tracer efflux by linear regression analysis.

The rate coefficient, k (s^{-1}), of the unidirectional efflux of tracer was used to calculate a permeability coefficient as $P = k \cdot (V \cdot A^{-1})$, where $(V \cdot A^{-1})$ is the ratio of the cell water volume

to the cell membrane area. Because transport of Cl^- and HCO_3^- saturates, the permeability coefficient is concentration dependent. We therefore use the term "apparent permeability" (P_{app}) to denote that the value of P refers to a given anion concentration (i.e., the concentration resulting from the physiological saline used). Data from the flux experiments are presented as means ± SE and were statistically evaluated by a two-factor (compound and oxygenation degree) ANOVA followed by the Tukey multiple-comparison test.

Hb H^+ Titration

RBCs from freshly drawn blood were washed three times in physiological saline. The packed RBCs were frozen in liquid N_2 and stored in a freezer at −80°C until use. Distilled water was added on thawing. The cell debris was removed by centrifugation, whereupon the hemolysate was passed three times through a mixed-bed ion-exchange column (Amberlite MB1, BDH) to remove cell solutes. The resulting isoionic Hb solution was brought to a KCl concentration of 0.1 mol/l, and total Hb concentration (cf. above) and methemoglobin (metHb) content (3) were measured. Hydrogen ion titrations were performed with a computer-controlled Radiometer TitraLab 90 titration system. Nine milliliters of Hb solution was transferred to the titration chamber, which was set at 30°C and closed with a lid. The Hb solution was magnetically stirred, and humidified pure O_2 (P_{O_2} = 730 mmHg) was supplied to the chamber to fully oxygenate the Hb. After 45 min of equilibration, the pH of the oxygenated isoionic Hb solution was recorded (Radiometer GK2401C combined pH electrode). The pH was subsequently elevated to about pH 9 by addition of freshly prepared 0.1 mol/l NaOH. After an additional 5 min of equilibration, titration with 0.1 mol/l HCl was initiated. The titration was continued until pH 5, resulting in ~250 data points per titration curve. A new 9-ml sample from the same Hb stock solution was then transferred to the chamber. After equilibration with O_2 (to verify the isoionic oxygenated Hb pH), the gas supply was shifted to humidified pure N_2 to deoxygenate the Hb. After 45 min of equilibration with N_2, the pH was brought to nine and the deoxygenated Hb solution was titrated with 0.1 mol/l HCl. Measurement of metHb after the titrations revealed that metHb formation during the titration procedure was insignificant.

RESULTS

Blood CO_2 Content, Acid-Base Status, and Hematology

Measurement of C_T in alligator blood equilibrated to 2% CO_2 (P_{CO_2} = 14.5 mmHg), 4% CO_2 (P_{CO_2} = 29 mmHg), and 7% CO_2 (P_{CO_2} = 50.8 mmHg) allowed the construction of carbon dioxide equilibrium curves for true plasma, whole blood, and RBCs (Fig. 1). C_T increased significantly with rising P_{CO_2} in all three compartments both when the blood was oxygenated and when it was deoxygenated. C_T in true plasma did not change significantly with oxygenation degree, whereas whole blood C_T was significantly higher in deoxygenated than in oxygenated blood, reflecting a large significant difference in C_T between deoxygenated and oxygenated RBCs (Fig. 1). At physiological P_{CO_2} (4% CO_2 = 29 mmHg), the difference between the mean C_T contents of deoxygenated and oxygenated whole blood was 3.21 mmol/l. When referenced to the prevailing blood Hb concentration ([Hb]) (Fig. 2), this corresponded to a Haldane effect in whole blood of 0.72 mmol CO_2/mmol Hb monomer.

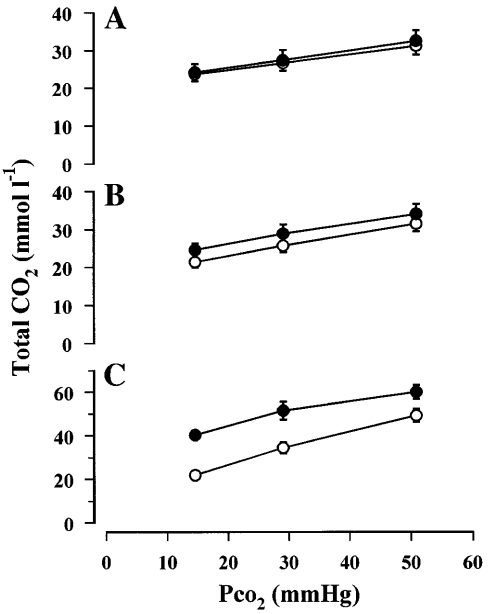

Fig. 1. CO_2 equilibrium curves for oxygenated (○) and deoxygenated (●) true plasma (*A*), whole blood (*B*), and red blood cells (RBCs; *C*) of the alligator (*Alligator mississippiensis*) at 30°C. Total CO_2 is given in mmol/l plasma, mmol/l blood, and mmol/l cell water for the 3 compartments, respectively. Means ± SE (n = 6).

Blood [Hb], Hct, and RBC [Hb] did not change significantly with oxygenation degree (Fig. 2). Mean Hct was 23.5%, and the tetrameric Hb concentration ([Hb_4]) of the blood was ~1.14 mmol/l (corresponding to a mean cellular [Hb_4] of 4.85 mmol/l RBC). The F_{H_2O} was close to 0.64 (Fig. 2). The N_{RBC} in alligator blood (millions/μl) was 0.698 ± 0.043, and the MCV at 4% CO_2 was 352 ± 11 μm^3.

Oxygenated blood equilibrated with a physiological CO_2 tension (4% CO_2 = 29 mmHg) had a pH_e of 7.56 and a plasma [HCO_3^-] of 25.7 mmol/l (Fig. 3). This acid-base status was similar to the in vivo arterial acid-base status in alligators at 30°C (11). Plasma lactate concentration was the same in oxygenated (0.9 ± 0.3 mmol/l) and deoxygenated (0.9 ± 0.2 mmol/l) blood. Plasma [HCO_3^-] and pH_e changed significantly in both oxygenated and deoxygenated blood when the CO_2 content of the equilibration gas was decreased to 2% CO_2 or increased to 7% CO_2 (Fig. 3). The true plasma nonbicarbonate buffer value ($\beta_{nb} = -\Delta[HCO_3^-]/\Delta pH_e$) was 15.7 $mmol \cdot l^{-1} \cdot pH\ unit^{-1}$ for oxygenated blood and 17.2 $mmol \cdot l^{-1} \cdot pH\ unit^{-1}$ for deoxygenated blood. The corresponding buffer values in whole blood (not illustrated) were 22.7 and 20.9 $mmol \cdot l^{-1} \cdot pH\ unit^{-1}$, respectively.

The pH_e did not differ significantly between oxygenated and deoxygenated blood at any of the CO_2 levels, and plasma [HCO_3^-] in deoxygenated blood was only slightly higher than in oxygenated blood (Fig. 3).

RBC CO_2 Content and Acid-Base Status

Elevating the CO_2 level from 2 to 4% and further to 7% CO_2 caused significant increases in the apparent

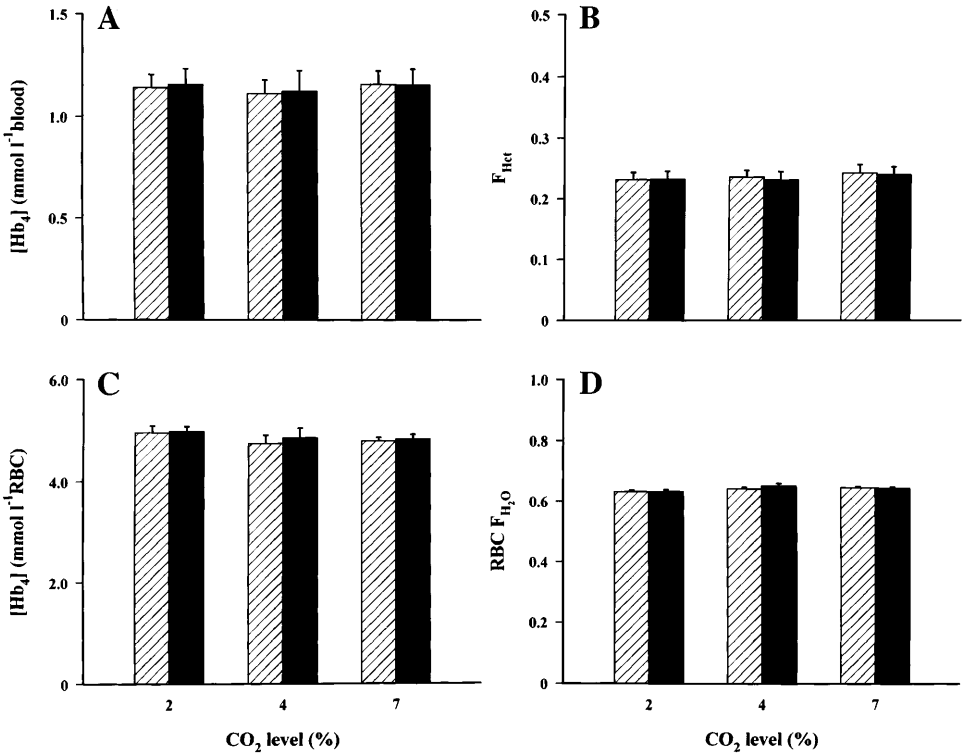

Fig. 2. Whole blood tetrameric Hb concentration ([Hb_4]; *A*), fractional hematocrit (F_{Hct}; *B*), mean cellular Hb concentration (*C*), and fractional water content (F_{H_2O}; *D*) of RBCs in oxygenated (hatched bars) and deoxygenated (solid bars) alligator blood at different CO_2 levels. Means ± SE (n = 6).

RBC bicarbonate concentration (in mmol/l cell water) and significant decreases in pH_i of both oxygenated and deoxygenated RBCs (Fig. 4*A*). The relationships between $[HCO_3^-]_{app}$ and pH_i were linear, revealing apparent intracellular β_{nb} values of 107.8 and 78.5 $mmol \cdot l^{-1} \cdot pH\ unit^{-1}$ in oxygenated and deoxygenated RBCs, respectively. Deoxygenation caused a pronounced increase in $[HCO_3^-]_{app}$ inside the RBCs (Fig. 4*A*), showing a large oxygenation-linked change in the RBC CO_2 binding capacity. The rise in $[HCO_3^-]_{app}$ observed in the alligator was unusual because there was no change in pH_i at any CO_2 level (Fig. 4*A*). If the improved CO_2 binding capacity on deoxygenation (Haldane effect) mainly had been a consequence of oxygenation-linked H^+ binding (as in other vertebrates), then the uptake of H^+ on deoxygenation would drive the CO_2 hydration equilibrium reaction toward HCO_3^- formation, leading to a rise in both erythrocytic $[HCO_3^-]$ and pH_i (*path b* in Fig. 4*A*). If oxygenation-linked HCO_3^- binding occurred but oxylabile H^+ binding was absent, then the RBC CO_2 binding capacity would also increase on deoxygenation but pH_i would decrease as result of the H^+ formed by CO_2 hydration. The actual data (Fig. 4*A*) suggest that in the alligator the binding of HCO_3^- to Hb on deoxygenation is balanced by an approximately equal oxylabile binding of H^+, leaving pH_i unchanged.

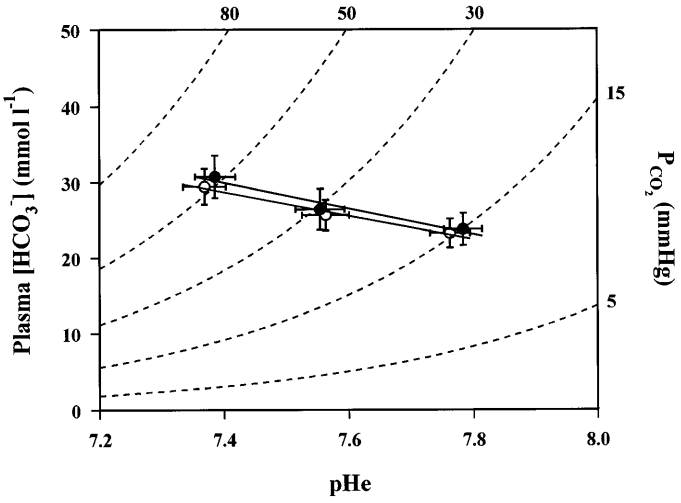

Fig. 3. True plasma HCO_3^- concentration ($[HCO_3^-]$) vs. extracellular pH (pH_e) in oxygenated (○) and deoxygenated (●) blood of the alligator (*Alligator mississippiensis*) at 30°C. Dotted lines are iso-P_{CO_2} curves calculated from the Henderson-Hasselbalch equation, using experimentally determined pK′ values (cf. MATERIALS AND METHODS). Means ± SE (n = 6).

When the intracellular $[HCO_3^-]_{app}$ was referred to the [Hb_4], it was evident that the difference in $[HCO_3^-]_{app}$/[Hb_4] between deoxygenated and oxygenated RBCs was close to two (Fig. 4*B*), suggesting binding of two HCO_3^- equivalents per Hb tetramer on deoxygenation. The change in $[HCO_3^-]_{app}$/[Hb_4] on deoxygenation was, however, pH dependent, being ~2.3 at pH_i 7.4 and ~1.5 at pH_i 7.2 (Fig. 4*B*). The slopes of the linear relationships between $[HCO_3^-]_{app}$/[Hb_4] and pH_i (Fig. 4*B*) revealed apparent Hb-specific buffer values of 15.1 and 11.2 $mol \cdot mol\ Hb_4^{-1} \cdot pH\ unit^{-1}$ in oxygenated and deoxygenated RBCs, respectively.

Red cell pH_i did not change significantly with oxygenation degree, whereby the relationship between pH_i and pH_e was the same for oxygenated and deoxygenated blood (Fig. 5*A*). The linear relationship between pH_i and pH_e had a slope, $\Delta pH_i/\Delta pH_e$, of 0.60 (Fig. 5*A*). The distribution ratio of H^+ across the red cell membrane ($rH^+ = [H^+]_e/[H^+]_i = 10^{pH_i - pH_e}$) was linearly related to pH_e, with a slope of −0.50 (Fig. 5*B*). The apparent distribution ratio of bicarbonate ($[HCO_3^-]_{i\,app}$/

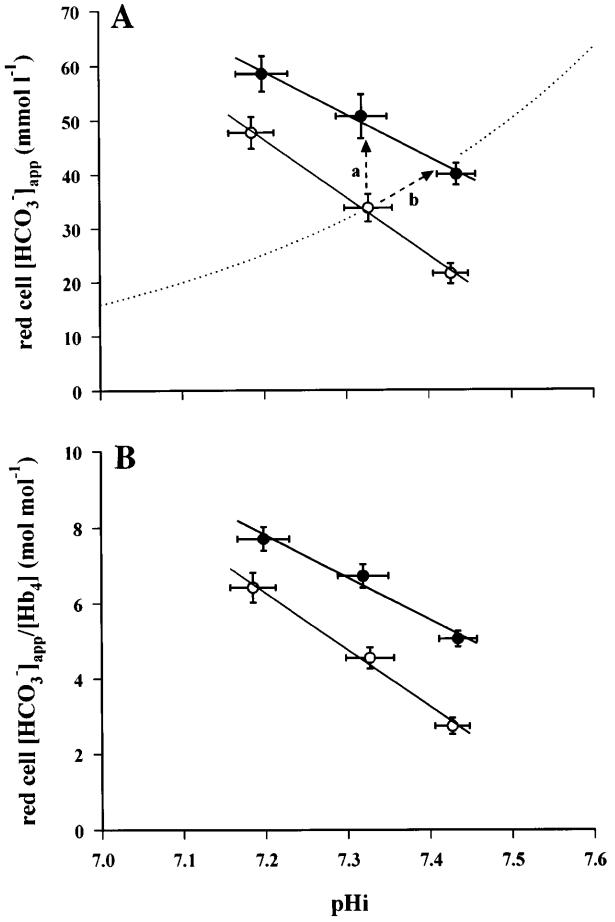

Fig. 4. *A*: apparent concentration (in mmol/l cell water) of bicarbonate (i.e., total CO_2 minus dissolved CO_2) as function of intracellular pH (pH_i) in oxygenated (○) and deoxygenated (●) RBCs of the alligator. *B*: ratio between apparent $[HCO_3^-]$ ($[HCO_3^-]_{app}$) and $[Hb_4]$ as a function of pH_i in oxygenated (○) and deoxygenated (●) RBCs from the alligator. Means ± SE (n = 6). *Arrow a* in *A* indicates actual change on deoxygenation at 4% CO_2. *Arrow b* is a hypothetical path along a tentative iso-P_{CO_2} curve (dotted curve), which should have been followed if HCO_3^- binding to the Hb had been absent and the difference between oxygenated and deoxygenated RBCs had been due to oxygenation-linked H^+ binding (see *RBC CO_2 Content and Acid-Base Status* for further explanation).

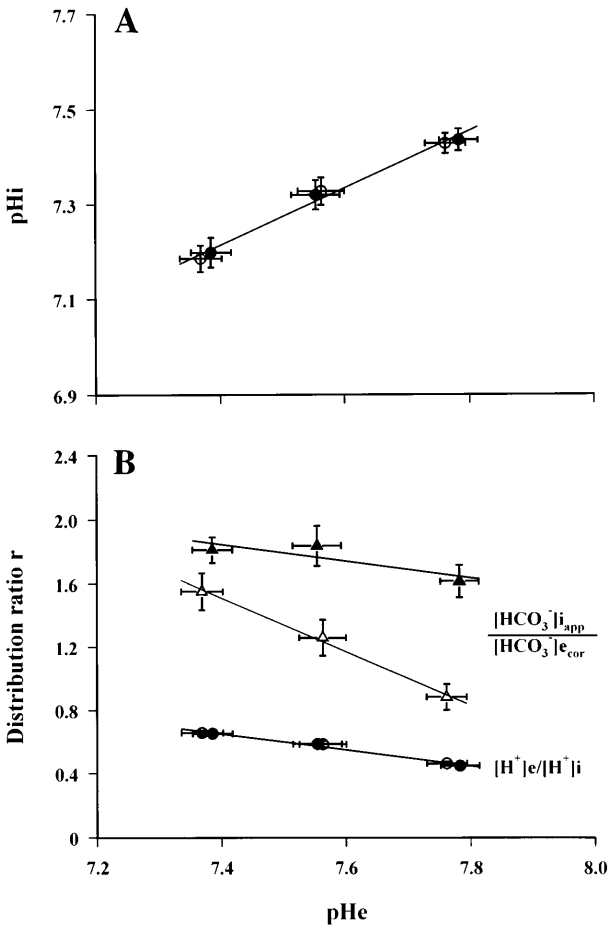

Fig. 5. *A*: relationship between RBC pH_i and pH_e in oxygenated (○) and deoxygenated (●) alligator blood. *B*: pH_e dependencies of the distribution ratio of H^+ and the apparent distribution ratio of bicarbonate across the RBC membrane in oxygenated (open symbols) and deoxygenated (closed symbols) alligator blood. Means ± SE (n = 6).

$[HCO_3^-]_{e\,cor}$, where $[HCO_3^-]_{e\,cor}$ is plasma $[HCO_3^-]$ corrected to mmol/l H_2O, assuming a plasma water content of 94%) was much higher than rH^+ and r values for bicarbonate in deoxygenated blood were significantly above those in oxygenated blood (Fig. 5*B*). Due to the very high intracellular $[HCO_3^-]_{app}$ (Fig. 4A), all apparent r values for bicarbonate, except for oxygenated blood at high pH_e, were >1, reflecting the unusual feature of larger intra- than extracellular values of $[HCO_3^-]_{app}$. The apparent r values for HCO_3^- were linearly related to pH_e (Fig. 5*B*). In deoxygenated blood the slope was −0.52 (i.e., similar to that for H^+), whereas it was −1.7 in oxygenated blood (Fig. 5*B*).

Partitioning of Total CO_2 in Deoxygenated RBCs

It was possible to analyze the quantitative contribution of different forms of carbon dioxide to C_T in deoxygenated RBCs, where the CO_2 content was maximal. Free CO_2 (i.e., dissolved molecular CO_2) constituted only a minor fraction of C_T (Fig. 6). The apparent bicarbonate concentration (i.e., C_T minus free CO_2) is made up of free HCO_3^-, Hb-bound HCO_3^-, and carbamate. Significant band 3-mediated HCO_3^-/Cl^- exchange

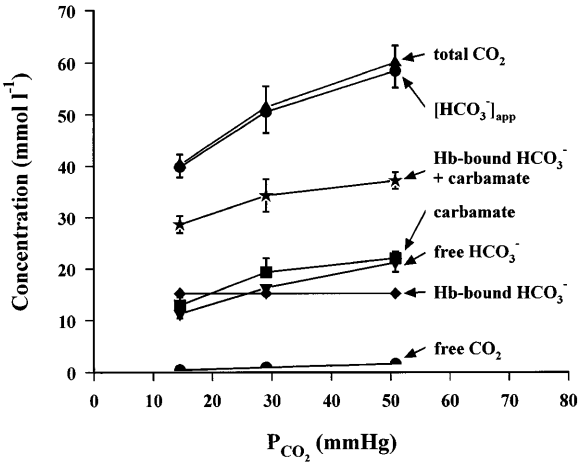

Fig. 6. Partitioning of total CO_2 into various forms of carbon dioxide in deoxygenated alligator RBCs. Concentrations are given in mmol/l cell water. See *Partitioning of Total CO_2 in Deoxygenated RBCs* for further explanation.

activity in alligator RBCs (cf. below) should ensure that free HCO_3^- and H^+ were passively distributed across the RBC membrane. Thus on the assumption that the distribution ratios for free HCO_3^- and H^+ were inversely equal, the concentration of free HCO_3^- in the water phase of the RBCs was estimated as the product between rH^+ and plasma $[HCO_3^-]$ (converted to mmol/l plasma water, using a plasma water content of 94%). $[HCO_3^-]_{app}$ minus free $[HCO_3^-]$ then gave the sum of Hb-bound HCO_3^- and carbamate. If each deoxygenated Hb tetramer was assumed to bind two HCO_3^- molecules over the pH/P_{CO_2} interval here considered, the concentration of Hb-bound $[HCO_3^-]$ was $2[Hb_4]_i/F_{H_2O}$ (the unit for $[Hb_4]_i$ is mmol/l RBC, and division with F_{H_2O} converts it to mmol/l cell water). The amount of carbamate was subsequently estimated as

$$[\text{carbamate}] = [HCO_3^-]_{app} - [HCO_3^-]_{free} - [HCO_3^-]_{Hbbound}$$

The analysis suggested that the amounts of free HCO_3^-, Hb-bound HCO_3^-, and carbamate were about equal in deoxygenated alligator RBCs at physiological P_{CO_2} (Fig. 6).

RBC HCO_3^-, Cl^-, and H_2O Permeabilities

Examples of Cl^-, HCO_3^-, and H_2O efflux under self-exchange conditions are shown in the semilogarithmic plot of Fig. 7. The tracer efflux curves were linear for all three compounds, allowing determination of the rate constants for the unidirectional effluxes by linear regression analysis. The mean *k* values for tracer efflux of Cl^-, HCO_3^-, and H_2O in oxygenated RBCs were 6.4, 14.2, and 44.1 s^{-1} respectively, all values being significantly different (Fig. 8*A*). Deoxygenation did not affect *k* for Cl^- and HCO_3^- (Fig. 8*A*). For water, however, the *k* value in deoxygenated RBCs was significantly lower than in oxygenated RBCs (Fig. 8*A*).

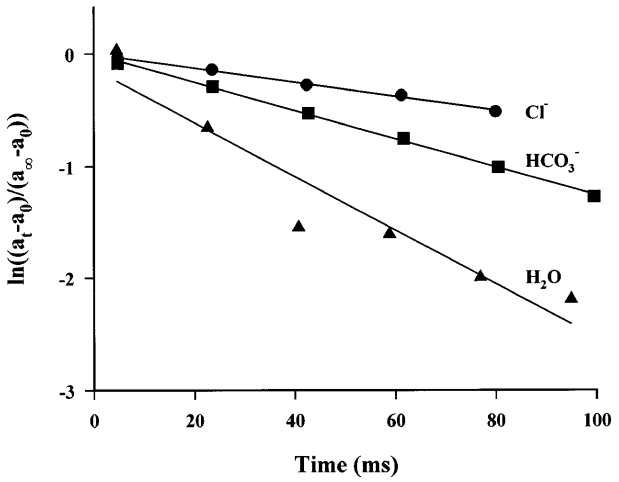

Fig. 7. Typical examples of $^{36}Cl^-$, $[^{14}C]HCO_3^-$, and ^3H_2O efflux from deoxygenated alligator RBCs under self-exchange conditions (30°C, pH 7.6). *Ordinate* represents fraction of tracer that remains in the cells at time *t*. a_t, a_0, and a_∞ denote extracellular radioactivity at *time t*, *time 0*, and at equilibrium. Linearity of the curves in the semilogarithmic plot indicates that the efflux follows a monoexponential course, and the slope of the curves hence equals the negative value of the rate coefficient *k* (s^{-1}).

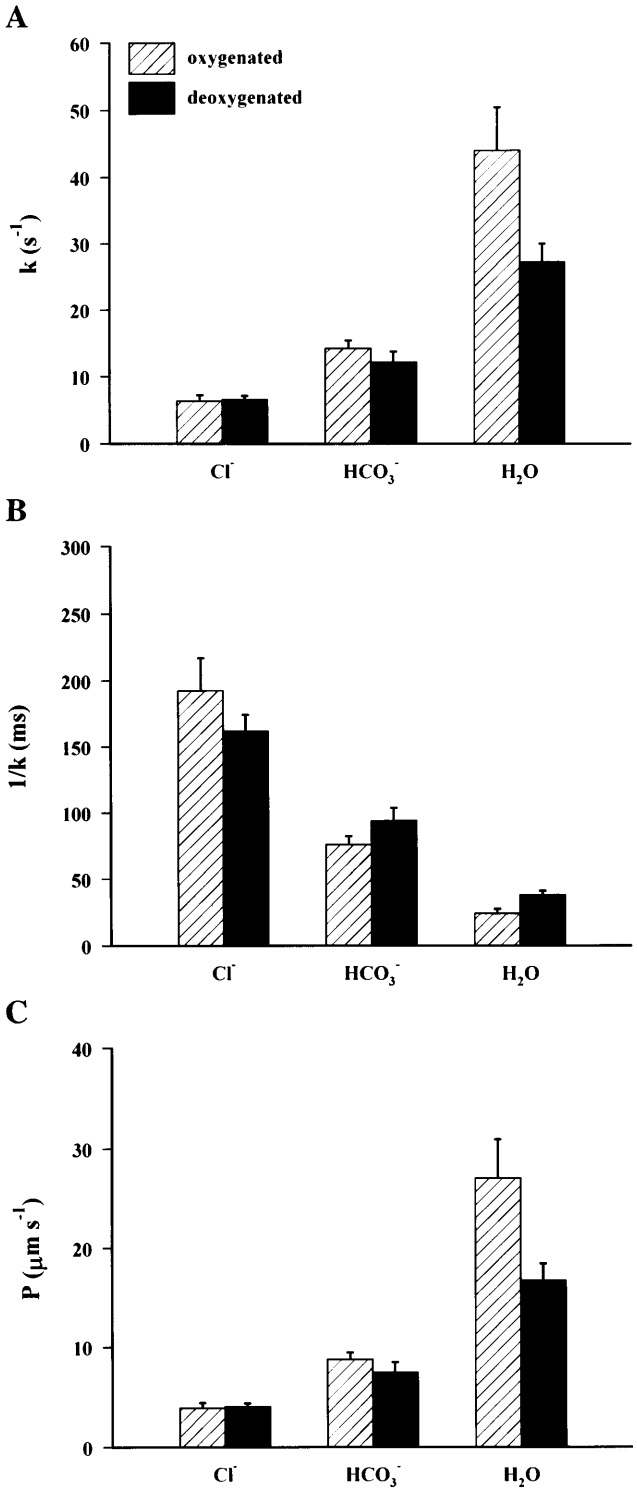

Fig. 8. Transport parameters in oxygenated (hatched bars) and deoxygenated (solid bars) alligator RBCs. *A*: rate coefficients (*k*) for the unidirectional efflux of Cl^-, HCO_3^-, and H_2O under self-exchange conditions. *B*: times required for 63% equilibration (1/*k*). *C*: apparent permeabilities (*P*) for Cl^- at $[Cl^-]_e$ = 110 mM and HCO_3^- at $[HCO_3^-]$ = 25 mM, and the diffusional H_2O permeability. Means ± SE (no. oxygenated/no. deoxygenated: Cl^-, 14/10; HCO_3^-, 11/10; H_2O, 4/4).

The presence of DNDS at 2.5 mmol/l reduced *k* for unidirectional $^{36}Cl^-$ efflux by 94% and 30 μmol/l phloretin inhibited the transport by >99%.

The time required for 63% equilibration of the fluxes (i.e., 1/*k*) varied from 192 ms for Cl^- in oxygenated RBCs to 24 ms for water in oxygenated RBCs (cf. Fig 8*B*).

The apparent membrane permeabilities for Cl^- and HCO_3^- and the diffusive H_2O permeability were evaluated from the *k* values and the measured MCV of 352 μm^3, a fractional RBC water content of 0.64 (Fig. 2*D*), and an estimated membrane area (A_m) of 367 μm^2. A_m was evaluated by assuming that the elliptical alligator RBCs were geometrically similar to fish RBCs and then calculating A_m as the average of the two values resulting from considering the RBC as being either an ellipsoid or two elliptical surfaces separated by a marginal band (17). The apparent Cl^- permeability was ~4 μm/s in both oxygenated and deoxygenated RBCs (Fig. 8*C*). The P_{app} for bicarbonate was significantly higher, being approximately the double of P_{Cl} (Fig. 8*C*). The diffusive water permeability was significantly higher than the values for Cl^- and HCO_3^- and the water permeability was significantly higher in oxygenated than in deoxygenated RBCs (Fig. 8*C*).

Hb H^+ Binding Properties

H^+ titration curves, revealing proton charge Z_H (mol H^+/mol Hb_4) as function of pH, of oxygenated and deoxygenated alligator Hb in 0.1 M KCl are shown in Fig. 9*A*. The vertical distance between the titration curves gives the fixed acid Haldane effect. At physiological pH values, alligator Hb took up protons on deoxygenation, and the number of H^+ taken up at constant pH (ΔZ_H, mol H^+/mol tetramer) reached a maximum ($\Delta Z_{H\,max}$) of 1.6 at pH 7.2. The first derivative of the titration curves ($-dZ_H/dpH$) yielded the buffer values (mol $H^+ \cdot$ mol tetramer$^{-1} \cdot$ pH unit^{-1}) for the oxygenated and deoxygenated Hb conformations. The buffer values varied with pH and with protein conformation (Fig. 9*B*). At pH 7.3 (which corresponds to physiological red cell pH_i at rest) the buffer values were 11.6 and 11.9 for oxygenated and deoxygenated Hb, respectively.

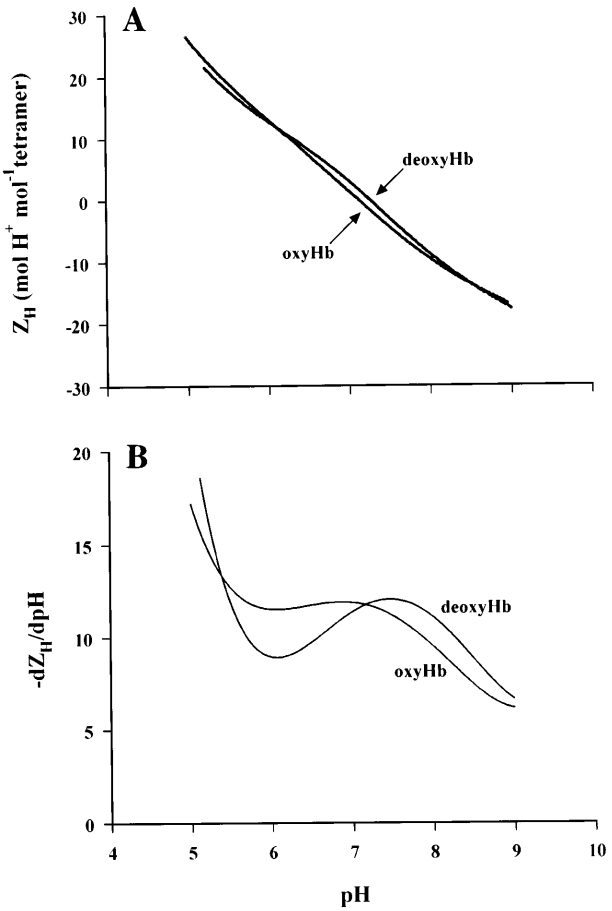

Fig. 9. Hydrogen ion equilibria of stripped alligator Hb in 0.1 mol/l KCl. *A*: net H^+ charge (Z_H, mol H^+/mol tetramer) as function of pH in oxygenated and deoxygenated Hb solutions. *B*: buffer values ($-dZ_H$/dpH, mol $H^+ \cdot$ mol^{-1} tetramer $\cdot$ pH unit^{-1}) for oxygenated and deoxygenated Hb as function of pH. Hb was kept oxygenated by equilibration with pure O_2 and was deoxygenated with pure N_2. Tetrameric Hb concentration = 0.21 mmol/l; temperature = 30°C.

DISCUSSION

HCO_3^- Binding to Hb in Intact RBCs

Studies at the molecular level show that two HCO_3^- molecules are bound to crocodilian Hb on deoxygenation (1, 21). The present study verifies this oxygenation-linked HCO_3^- binding in intact alligator RBCs (Fig. 4*B*). The improved CO_2 binding capacity of deoxygenated RBCs can be attributed to HCO_3^- binding to deoxygenated Hb and not merely to oxygenation-linked H^+ binding (as in other vertebrates), because the increase in $[HCO_3^-]_{app}$ at constant P_{CO_2} occurred without a change in pH_i (cf. the explanation given in RESULTS).

The difference in the ratio $[HCO_3^-]_{app}/[Hb_4]$ between deoxygenated and oxygenated RBCs was close to two but changed slightly with pH (Fig. 4*B*). Minor differences in the absolute value may have resulted from experimental uncertainties, because $\Delta[HCO_3^-]_{app}/[Hb_4]$ was assessed from measurement of several different parameters. The value slightly higher than two (i.e., 2.3) at high RBC pH_i could, however, also reflect a minor oxygenation-linked carbamate formation (i.e., preferential reaction of CO_2 with uncharged α-NH_2 groups in deoxygenated Hb). The value of $\Delta[HCO_3^-]_{app}/[Hb_4]$ between deoxygenated and oxygenated RBCs decreased to 1.5 at pH_i 7.2 (Fig. 4*B*). This finding suggests that HCO_3^- binds not only to deoxygenated Hb but also to oxygenated Hb when pH is decreased. Binding of HCO_3^- occurs to the quaternary T-structure of the Hb. At the highest pH (lowest P_{CO_2}) here examined, O_2 tension at half saturation (P_{50}) of alligator blood at 30°C is ~16 mmHg (extrapolated from data in Ref. 28). With this relatively high O_2 affinity, RBCs equilibrated with 98% air (P_{O_2} = 149.5 mmHg) primarily contain Hb with the R (oxy)-conformation, and oxygenation-linked HCO_3^- binding is absent. Lowering of pH, however, gradually shifts the R↔T equilibrium toward the T-state. P_{50} is ~40 mmHg (28) at the lowest pH here examined, and blood equilibrated with 93% air (P_{O_2} = 141.9 mmHg) therefore contains a significant quantity of T-structure Hb, leading to some

oxygenation-linked HCO_3^- binding in "oxygenated" RBCs.

The apparent distribution ratio of bicarbonate across the RBC membrane was higher than that for protons (Fig. 5*B*) because $[HCO_3^-]_{i\,app}$ includes not only free HCO_3^- but also carbamate and HCO_3^- bound to the Hb. If, however, in deoxygenated RBCs, two HCO_3^- molecules are bound to each Hb_4 molecule throughout the pH interval examined, then the slope of the relationship between *r* and pH_e should be similar for bicarbonate and protons. This indeed was the case (Fig. 5*B*). The steeper slope in oxygenated RBCs (Fig. 5*B*), can be attributed to a gradual HCO_3^- binding to oxygenated Hb as pH is lowered. Binding of HCO_3^- to Hb in oxygenated RBCs at low pH also influences the relationship between $[HCO_3^-]_{app}$ and pH_i (Fig. 4A). Thus in oxygenated RBCs the value of $-d[HCO_3^-]_{app}/dpH_i$ will be higher than that caused by nonbicarbonate buffering of H^+ per se. In deoxygenated RBCs, $-d[HCO_3^-]_{app}/dpH_i$ can be directly attributed to nonbicarbonate buffering.

H^+ Binding Properties and Red Cell pH

The buffer value per unit of Hb in hemolyzed oxygenated alligator RBCs is higher than in man and some lizards (10). The buffer value determined by CO_2 titration of oxygenated blood is potentially influenced by HCO_3^- binding to oxygenated Hb at low pH values (cf. above). The buffer value is, however, also high in deoxygenated RBCs (Fig. 4). Direct H^+ titration of alligator Hb revealed buffer values of 11.6 and 11.9 mol $H^+ \cdot$ mol $Hb_4^{-1} \cdot$ pH unit^{-1} for oxygenated and deoxygenated Hb at pH 7.3 (Fig. 9*B*), matching the Hb-specific buffer value of 11.2 mol $\cdot$ mol$^{-1} \cdot$ pH unit^{-1} determined in deoxygenated RBCs (Fig. 4*B*). The groups that are titrated between pH 6 and 9 are primarily the α-amino groups and the imidazole group of histidine residues (25). The acetylation of the β-chain α-amino group in alligator Hb (19) means that only the two α-chain α-amino groups can exchange protons. Alligator Hb, however, has 12 His residues in the α-chain and 13 His residues in the β-chain (19), giving a total of 50 His residues per tetramer, which is a high number among vertebrates (16). Not all His residues in the Hb molecule can be titrated but there is in general good correlation between the number of His residues and magnitude of buffer values (16). The relatively high buffer value of alligator Hb is therefore to be expected from the amino acid composition of the protein. The buffer value of alligator Hb at physiological pH is comparable to that of the elasmobranch *Squalus acanthias*, slightly higher than buffer values in most mammalian Hbs and much higher than buffer values in teleost Hbs, which have low histidine contents (16). When pH is decreased below pH 6, all titratable imidazole and α-amino groups have become positively charged. The groups titrated are now primarily the carboxyl groups of aspartic acid and glutamic acid residues. While pH is decreased toward pH 5, the buffer values increased above values observed at physiological pH (Fig. 9*A*). This is consistent with the high Glu (34/tetramer) and Asp (30/tetramer) content deduced from the primary structure af alligator Hb (19).

The proton uptake on deoxygenation reached a maximum of 1.6 mol H^+/mol Hb tetramer in alligator Hb. This value is higher than that of elasmobranch Hb, comparable to that of some mammalian Hbs, and lower than that of teleost fish (16). The $\Delta Z_{H\,max}$ of 1.6 at pH 7.2 in alligator Hb is similar to the ΔZ_H value of 1.51 in caiman Hb (1).

Normally, the uptake/release of H^+ on deoxygenation/oxygenation causes pH_i changes, the magnitudes of which depend on the amount of H^+ exchanged and the intracellular buffer capacity. In human blood ΔpH_i between deoxygenated and oxygenated RBCs is 0.03–0.05 pH units (23) and in teleost (that have high ΔZ_H values and low buffer values) it can be up to 0.35 pH units (15). In alligator RBCs, pH_i was not affected by changes in oxygenation degree (Fig. 5*A*). The important feature that distinguishes crocodilian RBCs from other vertebrates is the oxygenation-linked binding of both H^+ and HCO_3^- to the Hb. The amounts of H^+ and HCO_3^- taken up on deoxygenation (or released on oxygenation) are about equal in the alligator, which is also the case in the caiman (1). The oxylabile protons therefore balance the H^+ formed in the CO_2 hydration reaction as result of HCO_3^- binding to the Hb, and pH_i is not changed. Furthermore, if minor differences are present in the amounts of H^+ and HCO_3^- bound, the high intracellular buffer capacity will strongly limit pH_i changes.

Carbamate Formation

Partitioning of C_T in deoxygenated RBCs suggests that the amounts of free HCO_3^-, Hb-bound HCO_3^-, and carbamate were about equal at physiological P_{CO_2} (Fig. 6). With the Hb binding two HCO_3^-, this indicates that the number of carbamate groups per Hb tetramer is also about two in the alligator. Carbamate formation is possible at NH_2-terminal α-amino groups and at the ε-amino group of lysine residues (13). The extent of carbamate formation at lysine residues is normally small at physiological pH. This is because carbon dioxide only reacts with uncharged NH_2 groups. ε-Amino groups have a pK_a around 10 (13, 25) and are generally positively charged at physiological pH. However, with a total number of 44 lysine groups per tetramer in alligator Hb (19), it is possible that minor carbamate formation at some of the ε-amino groups adds up to a significant contribution. The α-amino groups, which have pK_a values close to physiological pH, normally contribute most to carbamate formation (13). In alligator Hb, the α-amino groups of the β-chains are acetylated (19, 21), whereby only the α-amino groups of the α-chains are available for carbamate formation. Carbamate formation at the NH_2-termini of α-chains may accordingly be extensive in alligator Hb.

The number of carbamate groups in caiman Hb (at pH 7.45, P_{CO_2} = 49 mmHg, 37°C, and ionic strength 0.1 M) was reported to be 0.9/tetramer (1). The estimated number of carbamate groups in the alligator is approximately double that in the caiman. This difference between the two crocodile species cannot be explained

by the total number of amino groups potentially available for carbamate formation. Caiman Hb has 46 Lys residues compared with 44 in alligator Hb, and the α-amino groups of the β-chains are not acetylated in the caiman (19). The NH_2-terminus of β-chains is, however, involved in HCO_3^- binding in both crocodilian Hbs, making carbamate formation unlikely at this site in both Hbs (21). A different carbamate formation in alligator and caiman Hb could result from differences in the molecular microenvironment of specific amino groups in the two Hbs, altering their pK_a values and thereby carbamate formation at a given pH. Alternatively, carbamate formation measured in intact RBCs (as with the alligator) may differ from that measured on purified Hb (as with the caiman).

The formation of carbamate does not appear to be oxygen-linked in caiman Hb (1). In the alligator, the major part of the carbamate was similarly not sensitive to oxygenation, although a minor oxygenation-linked component was indicated from the pH dependence of $\Delta[HCO_3^-]_{app}/[Hb_4]$ between deoxygenated and oxygenated RBCs (cf. above).

Haldane Effect

In other vertebrates, the improved CO_2 binding capacity on deoxygenation (Haldane effect) is due mainly to oxygenation-linked H^+ binding (the fixed acid Haldane effect) with variable contribution from oxylabile carbamate formation. In crocodiles, the origin of the Haldane effect is totally different, being mainly a consequence of oxygenation-linked HCO_3^- binding. The fixed acid Haldane effect is significant in the absence of CO_2 (Fig. 9*A*) but vanishes in the presence of CO_2 (1), because the hydrogen ions taken up by Hb balance those set free by formation and binding of HCO_3^-. The oxygenation-linked H^+ binding, however, nevertheless contributes to increased CO_2 carrying capacity. Oxygenation-linked HCO_3^- binding in the absence of oxylabile H^+ binding would be associated with a decrease in RBC pH_i and a smaller rise in $[HCO_3^-]_{app}$ on deoxygenation than when pH_i is constant.

The Haldane effect in alligator whole blood amounted to 0.72 mmol CO_2/mmol Hb monomer at constant physiological P_{CO_2}, which is about double the value in human blood, but slightly lower than the value of 0.9 in *Crocodylus porosus* (12). The value in both crocodilian species is close to the respiratory quotient (RQ). On the assumption that the relationship between HCO_3^- binding and Hb-O_2 saturation is linear, this implies that for every mole of O_2 released from Hb and consumed in tissue cells, the corresponding amount of CO_2 produced can be taken up by the blood without a change in P_{CO_2}. The O_2 and CO_2 transport at rest can therefore be predicted to proceed with minimal changes in P_{CO_2} between arterial and venous blood. This also suggests the absence of significant pH changes (Fig. 5*A*) between arterial and venous blood. In many vertebrates, the CO_2-induced pH decrease in tissue capillaries helps drive off O_2 via the Bohr effect. In the crocodiles, this effect is taken over by allosteric HCO_3^- binding.

RBC membrane permeability to Cl^-, HCO_3^-, and H_2O

Chloride and bicarbonate. The RBC volumes vary considerably among species. For that reason, transport rates, or rate coefficients (k, s^{-1}), cannot be used for comparison between species. The measured k values were converted into permeability coefficients by multiplication with the ratio of cell water volume to membrane area ($P = k \cdot V \cdot A^{-1}$) to allow an interspecies comparison. The apparent Cl^- permeability of the alligator RBC membrane at an external Cl^- concentration of 110 mM and 30°C was 4 μm/s (Fig. 8*C*). This value is only slightly lower than the value in human RBCs at 37°C (5.2 μm/s), and it is also close to values in fish at 15°C (1.7–5.6 μm/s) under otherwise comparable conditions (17). The P_{app} of alligator RBCs to HCO_3^- at an external concentration of 25 mM was 8 μm/s (Fig. 8*C*), which likewise compares well with the value of 7 μm/s in human RBCs at 38°C under similar "semiphysiological" conditions (calculated from Ref. 29). In fact, it is remarkable how relatively uniform the apparent permeabilities are despite large species differences in living style and physiological temperature. Anion exchange is a highly temperature-dependent process in RBCs from homeotherms such as humans and chicken (4, 7). On this basis, it may be profitable to study acute and chronic effects of temperature on anion transport in ectotherms to test whether the acute temperature sensitivity is reduced and whether temperature acclimation has an influence on the transport.

Information on band 3-mediated Cl^- and HCO_3^- transport is available for another reptile, the sea turtle (24). The capacity for anion exchange in the RBC of this species appears as high as in alligators. The high anion permeability found in alligator RBCs (Fig. 8) leads to the conclusion that the unique feature of HCO_3^- binding to Hb, which has evolved in the alligator, is not related to a low anion exchange capacity via band 3.

Human deoxygenated Hb binds to the cytoplasmic fragment of band 3 with a higher affinity than oxygenated Hb (27). This could potentially lead to an influence of oxygenation degree on band 3 anion transport kinetics (22). The kinetics of Cl^- and HCO_3^- transport were, however, similar in oxygenated and deoxygenated alligator RBCs under equilibrium conditions (Fig. 8). This is also the case in human RBCs and in RBCs from four different teleost species (17).

Water. The diffusive water permeability, P_d, was 27 μm/s in oxygenated alligator RBCs, but significantly reduced to 17 μm/s by deoxygenation (Fig. 8*C*). The value of P_d of oxygenated cells is similar to P_d of intact human RBCs or resealed red cell ghosts, while P_d of deoxygenated cells is close to the P_d of 10–12 μm/s obtained in human RBCs after maximum inhibition of the water transporting proteins with *p*-chloromercuribenzenesulfonate (5). To our knowledge this is the first study showing that oxygenation/deoxygenation has an effect on P_d. The origin of the effect is not clear. Colombo et al. (9) showed an allosteric binding of some 60 extra water molecules to Hb when it switches from the fully deoxygenated (T) state to the fully oxygenated

(R) state. The reduction of free intercellular water content is, however, small and also goes in the wrong direction to account for the change in P_d. Because the phenomenon apparently is not a general change of the solute permeability characteristics, it may be related to the transport pathways to water. By diffusion, water permeates the human RBC membrane through either the lipid phase or water transporting proteins in almost equal portions (5). If this also applies to alligator RBCs, deoxygenation may affect either the lipids or the proteinaceous water channels, closing either of the two pathways. A possible effect on the lipid pathway may be revealed by studying other RBCs such as chicken RBCs that lack the proteinaceous water channels (7).

CO_2 Transport in the Alligator

The unique CO_2 transporting properties of the blood in the alligator and other crocodiles give rise to a strategy for blood CO_2 transport that is fundamentally different from that in other vertebrates. The overall scheme for blood CO_2 transport arising from the present results is presented in Fig. 10.

As blood passes through tissue capillaries, metabolically produced CO_2 diffuses into the RBCs, where most of the CO_2 is rapidly hydrated to carbonic acid that dissociates to HCO_3^- and H^+. The formed HCO_3^- and H^+ are next bound in approximately equal amounts to the Hb in parallel with the release of oxygen. This is evidenced by the similar magnitudes of oxygenation-linked HCO_3^- (Fig. 4*B*) and H^+ (Fig. 9*A*) binding and by the constancy in pH_i on desaturation of the Hb (Figs. 4 and 5*A*). Only a minor fraction of the HCO_3^- is shifted to the plasma in exchange with Cl^-, as indicated by the insignificant rise in plasma C_T (Fig. 1) and $[HCO_3^-]$ (Fig. 3) on deoxygenation. This contrasts with the "mammalian strategy," where the contribution of anion exchange to elevate the CO_2-carrying capacity of blood is about equal to that of oxylabile H^+ binding and where most of the HCO_3^- formed in the RBCs is transported to the lungs as plasma HCO_3^- (29).

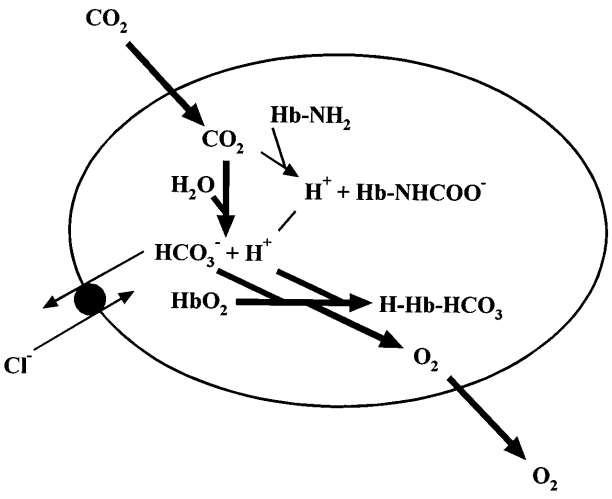

Fig. 10. CO_2 transport pattern in the alligator, showing the main processes and chemical reactions when CO_2 is added to blood in tissue capillaries. Thick arrows, major pathways; thin arrows, minor pathways. See *CO_2 Transport in the Alligator* for further explanation.

An almost stoichiometric binding of both HCO_3^- and H^+ when alligator Hb is deoxygenated means that the net charge on the Hb molecule changes little with oxygenation degree. This also contrasts with the situation in other vertebrates, where oxylabile H^+ binding decreases the nonpermeable negative charge carried by the Hb, giving rise to an increase in the Donnan-like distribution ratio of permeable ions and an associated swelling of the RBCs. Minimal oxygenation-linked changes in Hb charge in the alligator correlate with the absence of any influence of oxygenation degree on the distribution ratio of H^+ (Fig. 5*B*) and on Hct and red cell [Hb] (Fig. 2), the latter reflecting the minimal water fluxes and cell volume changes. Relative constancy in the Donnan-like distribution of permeable ions means that the concentration of free HCO_3^- changes little in both RBCs and plasma when CO_2 is taken up in tissue capillaries.

Dissolved CO_2 also changes little, because the magnitude of the Haldane effect is close to the RQ, allowing the produced CO_2 to be taken up with no significant change in P_{CO_2}.

Carbamate formation can be predicted to contribute little to arteriovenous CO_2 transport in crocodiles, because oxylabile carbamate formation is small and because the P_{CO_2} change between arterial and venous blood is minor. In humans, oxylabile carbamate accounts for some 13% of the CO_2 exchange (18).

The bulk of CO_2 taken up in tissue capillaries is accordingly carried by the blood within the RBCs, and primarily as HCO_3^- bound to Hb, until the blood enters the pulmonary capillaries where CO_2 is reformed and excreted (i.e., the reactions outlined in Fig. 10 proceed in the opposite direction). One other ancient vertebrate group, the lampreys, is also known to carry CO_2 primarily within the RBCs. In the lampreys, however, the mechanism is different from that in the crocodiles. Lamprey RBCs have a high pH_i, and the H^+ uptake on deoxygenation is large. The resulting high amount of HCO_3^- inside the RBCs exists as free HCO_3^- and is not shifted to plasma, because the RBC membrane is devoid of an anion exchange system (20, 26).

Although anion exchange is fast in most vertebrate RBCs, it is normally considered rate limiting for CO_2 exchange during exercise, where capillary transit time goes down and where disequilibria may develop as a result of an insufficient time to reach equilibrium between intracellular and extracellular C_T before the blood leaves the capillaries. In this regard the "crocodile strategy" of carrying CO_2 inside the RBCs may be superior. The binding and release of HCO_3^- from Hb are likely to be faster than anion exchange, so that disequilibria in arteries and veins are less likely to occur.

At first sight, it is surprising that alligator RBCs have a high capacity for anion exchange, when it is apparently not needed for optimizing blood CO_2 transport at normal RQ values. The chloride-bicarbonate shift is, however, also important for pH regulation by making the RBC buffer capacity available for extracel-

lular loads of acid (as observed after burst activity) or base (as observed after feeding when a large alkaline tide develops). Thus the anion exchange system is needed for transferring acid-base equivalents across the RBC membrane via the Jacobs-Stewart cycle. In this case, however, the extracellular CO_2 hydration/dehydration reaction becomes rate limiting (anion transport is much faster) unless carbonic anhydrase activity is available extracellularly.

Perspectives

The unique CO_2 transport scheme in the alligator illustrates that vertebrates can exploit different strategies of blood CO_2 transport as a result of differences in the functional properties of their Hbs. The latter comprises oxygenation-linked binding of HCO_3^- to Hb as well as major species differences in magnitudes of Haldane effects and buffer values (16). Allosteric binding of HCO_3^- to Hb has hitherto only been documented in crocodiles. This suggests that the property is rare, but does not exclude that it exists in other vertebrates. A possible discovery of allosteric HCO_3^- binding to Hb in other species and further studies on crocodiles under in vivo conditions may improve our understanding of its physiological significance. The apparent RBC permeability to anions in the alligator was similar to that in some fish species and in humans, despite differences in physiological temperature. This gives impulse to investigations of temperature adaption in band 3 function in ectothermic animals. Finally, the water permeability of alligator RBCs was oxygenation sensitive. This unexpected finding calls for studies on its ubiquity and functional importance.

We thank Drs. M. M. Vijayan and D. A. Syme for valuable technical support during the experiments.

The study was supported by a grant to the Danish Centre for Respiratory Adaptation from the Danish Natural Science Research Council.

Address for reprint requests: F. B. Jensen, Institute of Biology, Odense Univ., Campusvej 55, DK-5230 Odense M, Denmark.

Received 21 August 1997; accepted in final form 7 November 1997.

REFERENCES

1. **Bauer, C., M. Forster, G. Gros, A. Mosca, M. Perrella, H. S. Rollema, and D. Vogel.** Analysis of bicarbonate binding to crocodilian hemoglobin. *J. Biol. Chem*. 256: 8429–8435, 1981.
2. **Bauer, C., and W. Jelkmann.** Carbon dioxide governs the oxygen affinity of crocodile blood. *Nature* 269: 825–827, 1977.
3. **Benesch, R. E., R. Benesch, and S. Yung.** Equations for the spectrophotometric analysis of hemoglobin mixtures. *Anal. Biochem*. 55: 245–248, 1973.
4. **Brahm, J.** Temperature-dependent changes of chloride transport kinetics in human red cells. *J. Gen. Physiol*. 70: 283–306, 1977.
5. **Brahm, J.** Diffusional water permeability of human erythrocytes and their ghosts. *J. Gen. Physiol*. 79: 791–819, 1982.
6. **Brahm, J.** Transport measurement of anions, nonelectrolytes, and water in red blood cell and ghost systems. In: *Methods in Enzymology*, edited by B. Fleischer and S. Fleischer. New York: Academic, 1989, p. 160–175.
7. **Brahm, J., and J. O. Wieth.** Separate pathways for urea and water, and for chloride in chicken erythrocytes. *J. Physiol. (Lond.)* 266: 727–749, 1977.
8. **Cameron, J. N.** Rapid method for determination of total carbon dioxide in small blood samples. *J. Appl. Physiol*. 31: 632–634, 1971.
9. **Colombo, M. F., D. C. Rau, and V. A. Parsegian.** Protein solvation in allosteric regulation: a water effect on hemoglobin. *Science* 256: 655–659, 1992.
10. **Dill, D. B., and H. T. Edwards.** Properties of reptilian blood. IV. The alligator (*Alligator mississippiensis* Daudin). *J. Cell. Comp. Physiol*. 6: 243–254, 1935.
11. **Douse, M. A., and G. S. Mitchell.** Time course of temperature effects on arterial acid-base status in *Alligator mississippiensis*. *Respir. Physiol*. 83: 87–102, 1991.
12. **Grigg, G. C., and M. Cairncross.** Respiratory properties of the blood of *Crocodylus porosus*. *Respir. Physiol*. 41: 367–380, 1980.
13. **Gros, G., H. S. Rollema, and R. E. Forster.** The carbamate equilibrium of α- and ϵ-amino groups of human hemoglobin at 37°C. *J. Biol. Chem*. 256: 5471–5480, 1981.
14. **Heisler, N.** Parameters and methods in acid-base physiology. In: *Techniques in Comparative Respiratory Physiology. An Environmental Approach*, edited by C. R. Bridges and P. J. Butler. Cambridge, UK: Cambridge University Press, 1989, p. 305–332.
15. **Jensen, F. B.** Pronounced influence of Hb-O_2 saturation on red cell pH in tench blood in vivo and in vitro. *J. Exp. Zool*. 238: 119–124, 1986.
16. **Jensen, F. B.** Hydrogen ion equilibria in fish haemoglobins. *J. Exp. Biol*. 143: 225–234, 1989.
17. **Jensen, F. B., and J. Brahm.** Kinetics of chloride transport across fish red blood cell membranes. *J. Exp. Biol*. 198: 2237–2244, 1995.
18. **Klocke, R. A.** Velocity of CO_2 exchange in blood. *Annu. Rev. Physiol*. 50: 625–637, 1988.
19. **Leclercq, F., A. G. Schnek, G. Braunitzer, A. Stangl, and B. Schrank.** Direct reciprocal allosteric interaction of oxygen and hydrogen carbonate. Sequence of the haemoglobins of the caiman (*Caiman crocodylus*), the Nile crocodile (*Crocodylus niloticus*) and the Mississippi crocodile (*Alligator mississippiensis*). *Hoppe Seylers Z. Physiol. Chem*. 362: 1151–1158, 1981.
20. **Nikinmaa, M., S. Airaksinen, and L. V. Virkki.** Haemoglobin function in intact lamprey erythrocytes: interactions with membrane function in the regulation of gas transport and acid-base balance. *J. Exp. Biol*. 198: 2423–2430, 1995.
21. **Perutz, M. F., C. Bauer, G. Gros, F. Leclercq, C. Vandecasserie, A. G. Schnek, G. Braunitzer, A. E. Friday, and K. A. Joysey.** Allosteric regulation of crocodilian haemoglobin. *Nature* 291: 682–684, 1981.
22. **Salhany, J. M.** *Erythrocyte Band 3 Protein*. Boca Raton, FL: CRC, 1990.
23. **Siggaard-Andersen, O.** *The Acid-Base Status of the Blood*. Copenhagen: Munksgaard, 1976.
24. **Stabenau, E. K., C. G. Vanoye, and T. A. Heming.** Characteristics of the anion transport system in sea turtle erythrocytes. *Am. J. Physiol*. 261 (*Regulatory Integrative Comp. Physiol*. 30): R1218–R1225, 1991.
25. **Tanford, C.** The interpretation of hydrogen ion titration curves of proteins. *Adv. Protein Chem*. 17: 69–165, 1962.
26. **Tufts, B. L., and R. G. Boutilier.** The absence of rapid chloride/bicarbonate exchange in lamprey erythrocytes: implications for CO_2 transport and ion distributions between plasma and erythrocytes in the blood of *Petromyzon marinus*. *J. Exp. Biol*. 144: 565–576, 1989.
27. **Walder, J. A., R. Chatterjee, T. L. Steck, P. S. Low, G. F. Musso, E. T. Kaiser, P. H. Rogers, and A. Arnone.** The interaction of haemoglobin with the cytoplasmic domain of band 3 of the human erythrocyte membrane. *J. Biol. Chem*. 259: 10238–10246, 1984.
28. **Weber, R. E., and F. N. White.** Oxygen binding in alligator blood related to temperature, diving, and "alkaline tide." *Am. J. Physiol*. 251 (*Regulatory Integrative Comp. Physiol*. 20): R901–R908, 1986.
29. **Wieth, J. O., O. S. Andersen, J. Brahm, P. J. Bjerrum, and C. L. Borders, Jr.** Chloride-bicarbonate exchange in red blood cells: physiology of transport and chemical modification of binding sites. *Philos. Trans. R. Soc. Lond. B Biol. Sci*. 299: 383–399, 1982.